ELEMENTARY PARTICLES AND FIELDS
Experiment

Matrix Hodoscopes for the Oka (Protvino) and NA62 (SPS, CERN) Experimental Setups

E. N. Gushchin[1], **V. F. Kurshetsov**[2], **V. A. Lebedev**[1], **V. I. Romanovskiy**[2],
V. K. Semenov[2], **S. N. Filippov**[2], and **A. A. Khudyakov**[1]*

Received February 10, 2010; in final form, December 1, 2010

Abstract—The matrix hodoscope of the OKA experimental setup and a prototype of the hodoscope for the NA62 experiment are described. The design of both hodoscopes is presented. The requirements for the hodoscope prototype are listed, and the efficiency and the time resolution obtained on the basis of experimental data are quoted.

1. INTRODUCTION

1.1. OKA Experimental Setup

The OKA experimental setup [1, 2] is intended for precisely measuring parameters of rare kaon decays whose branching ratio falls within the range 10^{-3}–10^{-8}. A separated K^+ meson beam of momentum 12.7 GeV/c and and intensity $(4-6) \times 10^6$ K^+ mesons per spill is used at this setup.

The layout of the experimental setup is shown in Fig. 1. It includes scintillation counters (S); beam-spectrometer proportional chambers (BPC); gas Cherenkov counters ($\check{C}_{1,2}$), which are intended for identifying primary kaons; an 11-m-long decay volume equipped with a veto system; a wide-aperture magnetic spectrometer equipped with proportional chambers (PC), drift tubes (DT), and straw detectors (ST); a two-section multichannel gamma spectrometer (GAMS-EGS and GAMS-2000); a complete-absorption hadronic calorimeter (GDA-100); a matrix hodoscope (MH); and muon counters (MC).

1.2. NA62 Experimental Setup

The NA62 experimental setup [3] is intended primarily for measuring the branching ratio for the ultrarare decay $K^+ \to \pi^+ \nu \bar{\nu}$. This will make it possible to test Standard Model predictions to a high precision. The setup in question employs an unseparated 75-GeV/c beam of high intensity (3.3×10^{12} protons per spill).

The layout of the setup is presented in Fig. 2. The setup includes a GIGATRACKER beam spectrometer, an evacuated decay volume of length 80 m, a CEDAR differential Cherenkov counter for identifying primary kaons and a ring-imaging Cherenkov counter (RICH) for identifying pions, a pulsed spectrometer that employs straw detectors, a liquid-krypton calorimeter (LKr), and muon detectors (MuV).

2. MATRIX HODOSCOPE OF THE OKA EXPERIMENTAL SETUP

The matrix hodoscope is arranged downstream of the electromagnetic calorimeter in the immediate vicinity of it. In the schematic picture of the setup (see Fig. 1), these two units are denoted by MH and GAMS-2000, respectively. The hodoscope serves for solving the following problems.

First, it is intended for resolving the XY ambiguity since the pad hodoscope determines unambiguously the particle coordinate and since the setup does not involve inclined chambers.

The second task of the hodoscope is the time matching of the tracks, this making it possible to reject tracks associated with random coincidences.

In addition, the hodoscope may generate a multiplicity (number of actuated pads) trigger. This permits selecting decay channels featuring one or three charged particles in the final state.

[1]Institute for Nuclear Research, Russian Academy of Sciences, pr. Shestidesyatiletiya Oktyabrya 7a, Moscow, 117312 Russia.
[2]Institute for High Energy Physics, Protvino, Moscow oblast, 142284 Russia.
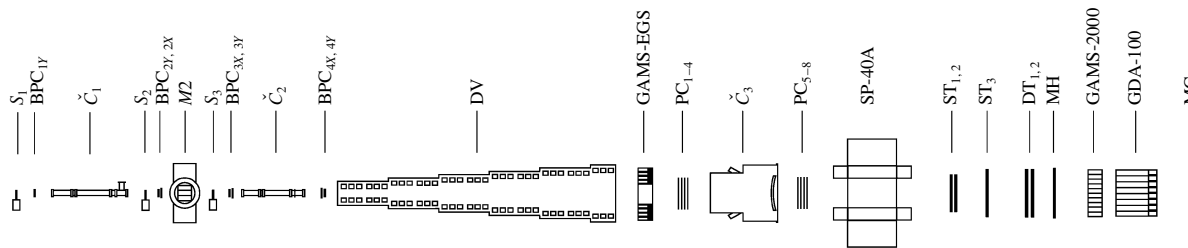*E-mail: aleksey.khudyakov@cern.ch

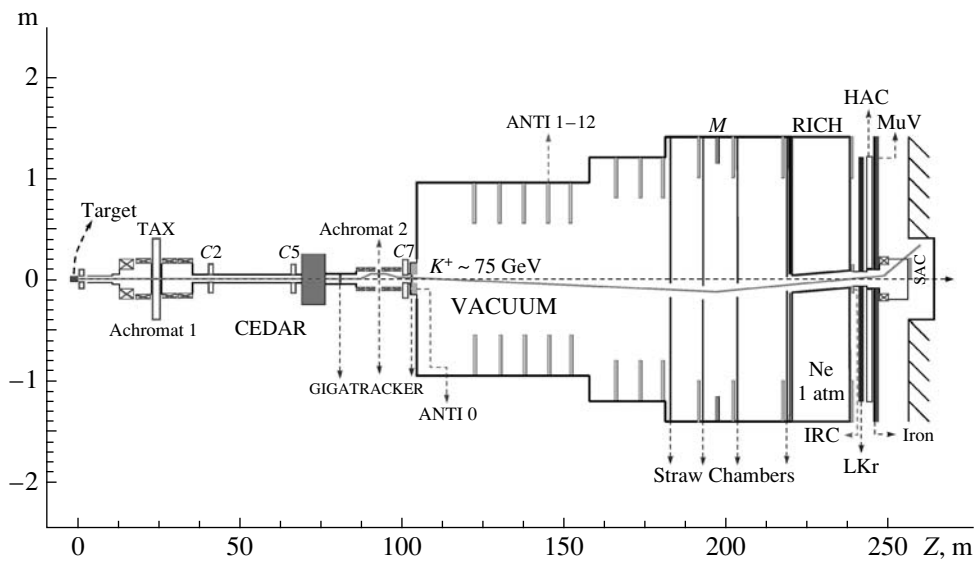**Fig. 1.** Layout of the OKA experimental setup.
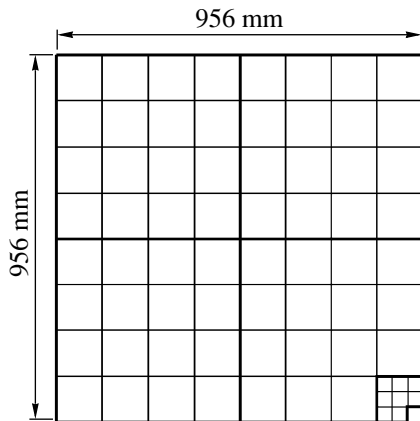

Fig. 2. Layout of the NA62 experimental setup.

Fig. 3. Schematic picture of one quadrant in the matrix hodoscope of the OKA experimental setup.

Fig. 4. Scintillation pad. An ultraviolet photodiode is fixed at the center of the pad.

2.1. Hodoscope Design

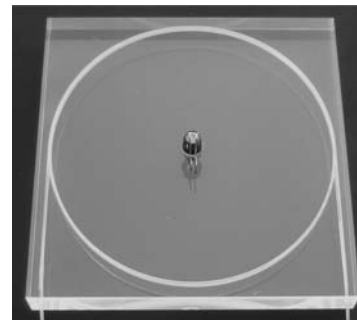The hodoscope consists of four quadrants, each containing 8×8 pads. The angular pad closest to the beam is replaced by an assembly of 3×3 pads, one of these being removed to let the beam propagate freely. The layout of the pad arrangement is shown in Fig. 3.

Each scintillation pad has the shape of a parallelepiped 120×120 mm^2 in cross-sectional area and 15 mm in thickness. Light collection is performed with the aid of a Y11(250)-MSJ spectrum-shifting fiber (Kuraray) 1 mm in diameter laid in a ring-shaped groove, where it makes 3.5 turns. In order to improve an optical contact, the fiber was glued to the groove
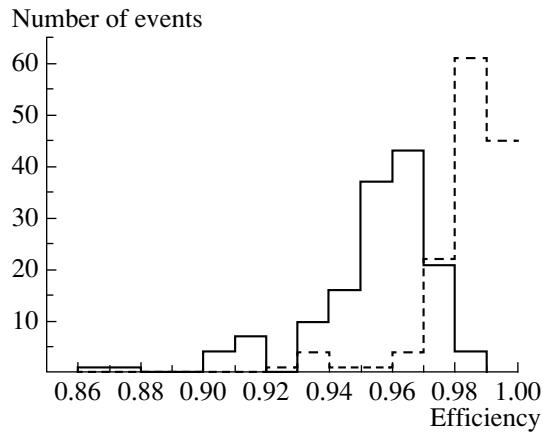
Number of events

Fig. 5. Distribution of the efficiency of matrix-hodoscope pads. The solid-line histogram is the distribution of the efficiency determined for one pad, while the dashed-line histogram corresponds to the entire hodoscope.

Number of events

Fig. 6. Distribution of the time of arrival of a pulse from the hodoscope.

Fig. 7. Photograph of the hodoscope during the process of assembling it.

with a BC-600 (Bicron) glue. Moreover, each pad was wrapped in a TYVEK light-reflecting coat in order to enhance light collection. A photograph of a scintillation pad is given in Fig. 4.

Scintillation light is recorded by means of avalanche photodiodes (APD). They have small dimensions, and their operation does not require a high voltage. This made it possible to arrange APDs directly on the scintillation pads. The APD internal amplification is about 10^6, which makes it possible to employ APDs without additional amplification [4].

Electronics generating a multiplicity trigger are mounted directly on the detector.

2.2. Hodoscope Efficiency

The efficiency of the matrix hodoscope was determined on the basis of data accumulated over the April run of 2009. One-prong events were selected for this. They can be reconstructed without using the matrix hodoscope. The efficiency of a pad was determined as follows: events for which the reconstructed track pointed to this pad were selected, and the ratio of the number of pad actuations to the number of events and the ratio of the number of events where there is at least one actuation in the hodoscope to their total number were estimated.

The first estimate is underrated: even if a track points to a pad, the particles involved could in fact miss the pad. Such events contribute to inefficiency. The second estimate is overrated since random actuations in other pads may mask inefficiency.

The distribution of the pads with respect to the efficiency determined by the above two methods is given in Fig. 5. The true efficiency lies between the two estimates and exceeds 95%.
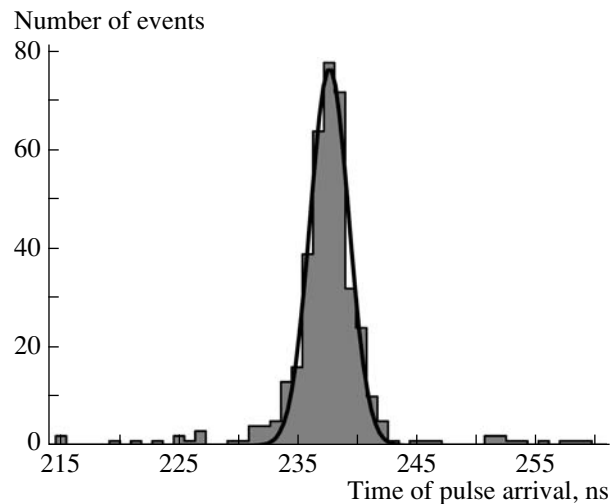
2.3. Time Resolution

Figure 6 shows the distribution of the time of arrival of a pulse from a matrix hodoscope. The numbers of channels of the cycled-memory register are plotted along the abscissa. A unit interval is 0.9 ns. The time resolution determined in this way is $\sigma_t = 1.8$ ns.

2.4. Results

The hodoscope operated successfully in the April and November runs of 2009. The data obtained within these periods were used to reconstruct multiprong events. A trigger for the number of charged secondaries was successfully tested in the November run.

3. MUON HODOSCOPE OF THE NA62 EXPERIMENTAL SETUP

The muon hodoscope (in the following, MuV, which stands for Muon Veto) enters into zero-level
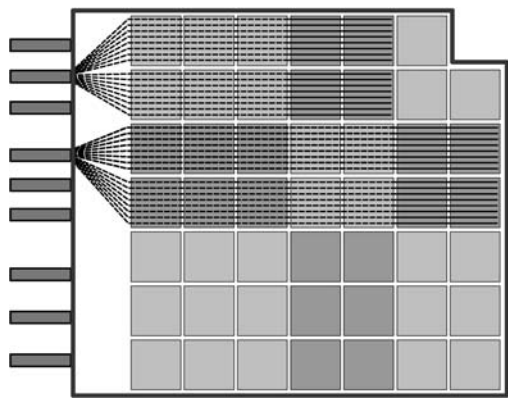
Fig. 8. Layout of the hodoscope. The pads are denoted by various grades of gray. The gaps between the pads are shown exclusively for the purpose of illustration—in fact, the pads fully overlap one another. Light collection from two pads is given. The light guides are represented by solid lines in the region an optical contact and by dashed lines in the region where they are light-insulated from the scintillator.

Fig. 9. Efficiency of the muon hodoscope. The region where triggering strips overlap one another is shaded. The dashed lines correspond to the boundaries of the hodoscope pads.

triggers and serves for suppressing muons from the decay $K^+ \to \mu^+\nu$ (Br $\approx 63\%$). Since the setup deals with an ultrahigh-intensity beam, the hodoscope must possess a high time resolution (about 1 ns) for minimizing the dead time of the setup. The muon-detection efficiency must be higher than 99% in order to suppress the muon background by a factor in excess of 100.

The hodoscope consists of four quadrants. A muon-hodoscope prototype consisting of one quadrant was manufactured and tested. Figure 7 shows a photograph of the hodoscope in the course of assembling it.

Each quadrant consists of nine pads having unequal dimensions. Each pad features two layers of scintillation plates 200×200 mm^2 in dimension. In the vicinity of the beam, the pads are 400×400 mm^2

Muon-hodoscope time resolution (in nanoseconds) measured for various photomultiplier tubes

N_{run}	Pad number					
	1*	2*	3	4*	5*	6
21288	1.93[1]	1.29[3]	1.71[2]	1.43[3]	1.16[1]	1.76[2]
21290	1.81[1]	1.16[2]	1.81[3]	1.53[3]	1.17[2]	1.74[1]
21292	1.77[1]	1.24[2]	1.80[3]	1.99[3]	1.18[2]	1.74[1]
21298	1.76[1]	1.25[1]	1.69[2]	1.52[2]	1.24[2]	1.73[1]

Note: An asterisk on the pad number indicates that the light guides were glued to the scintillator. The indices correspond to the following types of the photomultiplier tubes (PMT) used: (1) PMT-85, (2) Hamamatsu-R7899-20, and (3) PMT-115M.
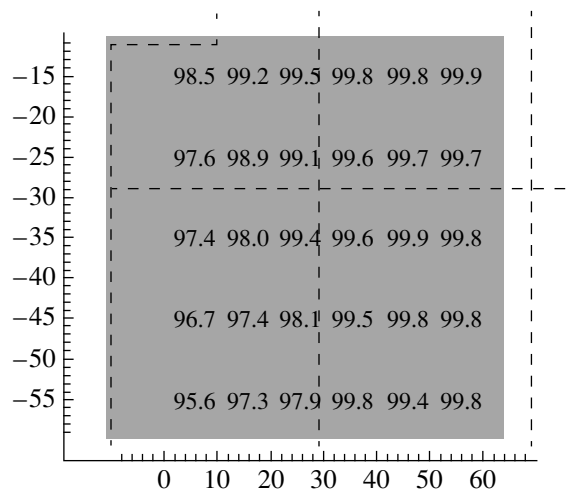
(or 2×2 plates) in dimension. Peripheral pads have larger dimensions, 400×600 and 600×600 mm^2 (2×3 and 3×3 plates, respectively), since the counting rate far off the beam is smaller. The layout of the hodoscope is given in Fig. 8. The pads are represented by different grades of gray.

Eight parallel grooves in which a spectrum-shifting fiber is laid is made in each scintillation plate. Within a single pad, this fiber is in light contact with a scintillator, whereupon it is brought out above the light-reflecting coat. All fibers from the same pad are connected to a single photomultiplier tube.

In the schematic picture in Fig. 8, the light guides are represented by solid lines, while the region where they are light-insulated from the scintillator is denoted by dashed lines.

3.1. Efficiency of MuV

In order to select muons, use was made of the strip muon hodoscope that remained from the NA48/2 experimental setup. Its two planes featuring mutually orthogonal strips are positioned upstream and downstream of MuV. Two strips of one plane and three strips of the other are used. The region of their overlap entirely lies within MuV.

In Fig. 9, the region where the strips overlap one another is represented by the gray square, while the boundaries between the MuV pads are shown by dashed lines. Only one-prong events were used to determine the required efficiency. The numbers in Fig. 9 stand for the efficiency of the hodoscope in percent versus the particle coordinate. A charged hodoscope was employed to obtain this efficiency.

3.2. Time Resolution of MuV

Before a test run, the light guides for four pads were glued to the scintillator in order to increase light accumulation and, accordingly, to improve the time resolution. The measurements were performed for three types of photomultiplier tubes (PMT): PMT-85, PMT-115M, and Hamamatsu-R7899-20. The time resolutions obtained on the basis of four runs are presented in the table.

From the table, one can see that the time resolution for the pads featuring glued light guides falls within the range 1.15−1.7 ns. For pads where light guides were not glued, it is poorer, amounting on average to 1.7 ns.

3.3. Results

In October 2009, a prototype of the muon hodoscope for the NA62 experiment was tested in a beam. The prototype revealed a high efficiency and a high time resolution that are sufficient for operation with the veto detector.

REFERENCES

1. V. F. Obraztsov and L. G. Landsberg, Nucl. Phys. B Proc. Suppl. **99B**, 257 (2001).
2. V. F. Obraztsov and L. G. Landsberg, hep-ex/0011033v1.
3. G. Anelli et al., CERN-SPSC-2009-24.
4. S. Filippov and E. Gushchin, Nucl. Instrum. Methods Phys. Res. A **610**, 404 (2009).

Translated by A. Isaakyan